http://www.hcplive.com/journals/family-practice-recertification/2015/june2015/why-does-a-12-year-old-have-enlarged-thymus-gland-causing-headaches-and-loss-of-vision

Why Does A 12-Year-Old Have Enlarged Thymus Gland Causing Headaches and Loss of Vision

Author: James D. Collins, MD

HISTORY

This is a 12-year-old male water polo player who presented with intermittent headaches associated with black floaters in his visual fields and loss of vision. (1). He experienced the symptoms during water polo when he positioned both arms above his head when stretching, or when he held a ball above his head while treading water. In addition, the patient stated that he found compressing with his right index finger a bump behind the manubrium in his suprasternal notch could actually cause him to “pass out”.

During these activities he visualized black spots bilaterally that progressed to temporary blindness. He also experienced right-sided headaches, tingling, and numbness of all fingers in his right hand, except for his thumb. (2) On occasion, he experienced blanching of his right hand. All of these episodes lasted for several seconds until he lowered his arms down from above his head. He did not experience syncope or loss of consciousness.

His initial workup from another institution included an EEG, MRI and MRA of the chest, as well as an ultrasound that were all negative. Thereafter, he was referred to an Ophthalmologist who suspected thoracic outlet syndrome and referred him to a vascular surgeon for evaluation.

PHYSICAL EXAMINATION

On examination, the patient had a blood pressure of 110/70 in his right arm that dropped to 70/40 with his arm raised. He had a resting heart rate of 24 beats per minute, a pulse of 78, and a temperature of 98.6. He weighed 90 pounds.

When the physician took the blood pressure, elevation of the right arm triggered complaints of pain over the right upper extremity, blurred vision, bilateral parietal headaches, as well as tingling and numbness of the right arm and hand. Adson’s maneuver was positive. The hand intrinsic, ulnar, and median muscles were markedly weaker on the right compared to the left. Reflexes in the biceps, triceps, and

brachioradialis were symmetric. A palpable “lump” was detected above the suprasternal notch.

Because the clinician suspected the clinical diagnosis of thoracic outlet syndrome, the patient was scheduled for repeat posterior and lateral chest radiographs and anterior posterior radiograph of the cervical spine with bilateral MRI, MRA, and MRV of the brachial plexus.

Radiographic findings

The posterior anterior (PA) chest radiograph (Figure 1) displays the head and neck leaning away from the painful right shoulder; anterior rotated heads of the clavicles over the posterior third intercostal spaces; drooping right shoulder as compared to the forward anterior rotated left, low right first rib as compared to the left first rib; an amorphous hazy density widening the mediastinum obscuring the lucency of the trachea down to the carina at the T6-T7 interspace.

The lateral chest radiograph cross references the PA chest (Figure 2) to display the forward shift of the cervicothoracic spine; narrowed thorax; mild kyphosis of the thoracic spine anterior bowing the body of the sternum: asymmetric first ribs backwardly displacing manubrium; hazy amorphous bulging soft tissue density the above the first ribs that inferiorly descends obscuring the trachea and arch of the aorta down below the region of the carina.

Diagnosis

1) Bilateral round shoulders, right greater than left.
2) Anterior superior mediastinal mass possibly one the four Ts-tumor (lymphoma), substernal thyroid, teratoma, and thymoma.
3) Mild concave right scoliosis of the cervicothoracic spine.

MAGNETIC RESONANCE FINDINGS

The thymus gland was enlarged splaying apart the brachiocephalic veins (Figure 3); manubrium backedwardly displacing the aorta and the great vessels (Figure 4), and the thymus gland compressing the left brachiocephalic vein against the backward aorta against the trachea (Figure 5). The 2D Time Of Flight MRA (magnetic resonance angiography), MRV (magnetic resonance venography) (Figure 6) cross referenced the T1 weighted images above to display the “cone shaped” compression of the inferior bicuspid valve within the right internal jugular vein with compression of the right brachiocephalic vein diminishing venous return into the superior vena cava and the backward manubrium compressing the left

brachiocephalic vein against the ascending aorta, left common carotid artery and the brachiocephalic trunk diminishing venous return from the left neck, supraclavicular fossa and shoulder.

Conclusions from bilateral MRI MRA MRV of the brachial plexus

1) Bilateral round shoulders, right greater than left.

2) Mild right concave cervicothoracic Kyphoscolisis of the thoracic spine on the upright chest straightens significantly secondary to the body weight on the MRI.

3) Bilateral enhanced thymus gland compression of the brachiocephalic veins as above described to form the superior vena cava, right brachiocephalic greater than left.

4) Mass effect from the enlarged thymus gland.

5) Bilateral costoclavicular compression (laxity of the sling/erector muscles- trapezius, levator scapulae, and the serratus anterior) of the bicuspid valves within the draining veins within the neck, supraclavicular fossae with lymphatics and compression of the subclavian and axillary arteries with binding nerves, right greter than left, particularly the right internal jugular and the two brachiocephalic veins.

DISCUSSION

The circulatory system is a closed system. The lymphatic tissues and organs include the thymus, bone marrow, lymphatic follicles, lymph nodes and the spleen, which are part of the circulatory system that collect and drain lymph from other tissues of the body, and are included in the definition of the immune system.

The thymus is irregularly shaped bilobed organ (Figure 7) that lies in the deep fascia of the neck, inferior to the thyroid gland. The thymus has a connective tissue capsule, a lymphocyte-rich cortex and a medulla rich in epithelial reticular cells. During fetal life the thymus is populated by stem lymphocytes from the liver. When blood cell formation moves from the liver to the bone marrow, the bone marrow becomes the source of stem lymphocytes in the thymus. It is in the thymus that these marrow-derived lymphocytes proliferate and differentiate into T cells, under the action of the lymphokine known as thymosin. As a source of T cells, the thymus is a key organ in the immune system. The thymus is relatively large in newborns and at puberty reaches its largest absolute size but is relatively small compared to the rest of the body's tissues. In later life it involutes and the reticular cells are replaced by

fatty degenerated-looking cells; there may be plasma cells as well.

Magnetic resonance imaging demonstrates vivid anatomical detail as in our patient that cannot be duplicated by any other modality (ie, CT or ultrasound).
However, MR can be coupled to other imaging Modalities such as plain radiographs of the chest to enhance pathological descriptions. Magnetic resonance imaging allows multiplane imaging without surgical dissection, giving the patient an alternative to surgery and invasive procedures that may endanger his health.

In patients with the clinical diagnosis of thoracic outlet syndrome (TOS), bilateral MRI of the brachial plexus displays the thymus as an intermediate gray proton density within the anterior mediastinum posterior to the manubrium sterni. In adolescent patients it extends into the anterior neck enveloping the brachiocephalic vein and artery. In adult and older patients it may be identified as an isolated grey proton-dense structure medial to the left carotid sheath. The gland downwardly displaces the proximal left brachiocephalic vein; backwardly displacing the aorta and the brachiocephalic trunk, and splays apart the carotid sheath as in our patient.

This patient for this presentation was selected because of a massive thymus gland in the anterior superior mediastinum on plain chest radiographs confirmed by bilateral MRI, MRA, MRV of the brachial plexus. The thymus gland extended above the manubrium enveloping displacing and compressing the brachiocephalic veins and brachiocephalic trunk enhancing costoclavicular compression of the draining veins within the neck and supraclavicular fossae.

The thymic mass effect altered fascial planes in the patient's neck and caused difficulty in breathing and sleeping. When he raised his arms overhead, he visualized black floaters with tingling and numbness of fingers and toes and hip pain reflecting impedance to venous return. When he used his fingers to depressed the thymus, he enhanced decrease in arterial, venous and lymphatic perfusion (ischemia) to and from the brachial plexus that triggered complaints.

Other possible etiologies of the patient's complaints were ruled out by the MRI/MRA/MRV. Our narrative presentation included statements and descriptions of images not displayed. A more extensive report for the patient's file was supported by all of the sequences including the above selected images. Unlike x-ray images, a diagnosis is not made
from a single plain film, although chest radiographs are correlated with the MRI, MRA, and MRV for a more accurate diagnosis. Since it is
not possible to present all of the images, those selected best demonstrated the pathology (3)

TAKE HOME MESSAGE

Posterior-anterior and lateral chest radiographs are essential for examination of the thorax on MRI, MRA and MRV. Upright x-rays provide display of 70% of normal and abnormal landmark anatomy because 30% of the x-ray beam is absorbed by the patient. In this patient, correlation of the chest radiograph findings with bilateral MRI, MRA, and MRV brachial plexus were required to allow for a more accurate diagnosis.

Knowledge of landmark anatomy allows the radiologist to consider different etiologies in patient complaints. When using magnetic resonance imaging, you never know what anomaly or abnormality will be displayed. (4, 5, 6)

FIGURE LEGENDS

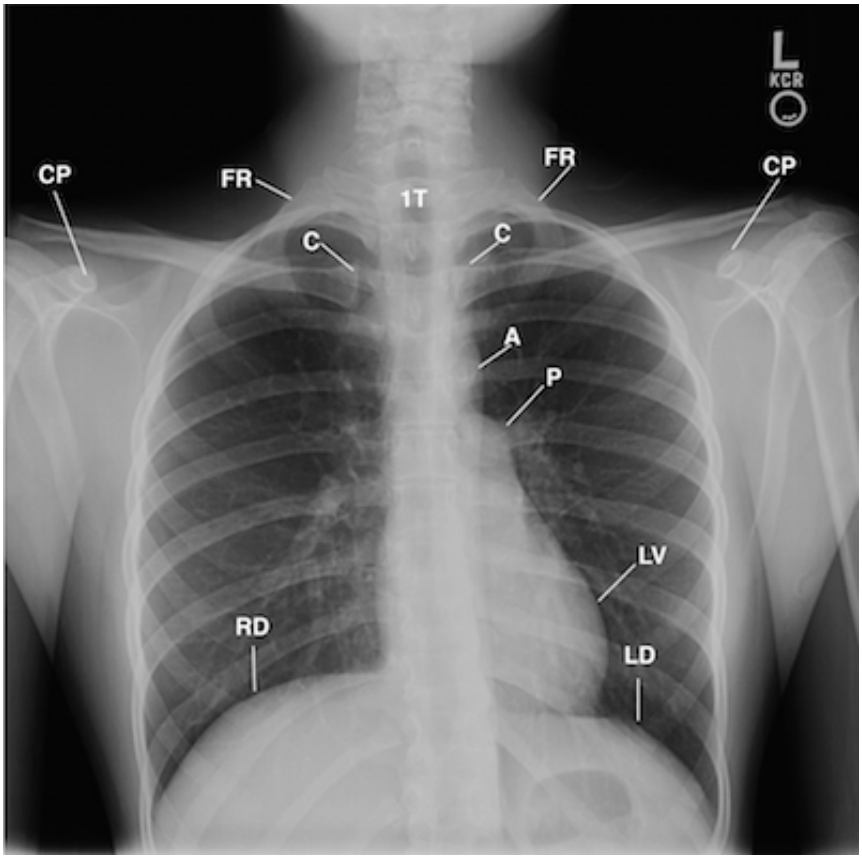

FIGURE 1. This is a posterior anterior (PA) chest radiograph that displays the head and neck leaning right; anterior rotated heads of the clavicles (C) over the posterior third intercostals spaces; drooping right shoulder as compared to the elevated forward anterior rotated left shoulder; right first rib (FR) lower than the left first rib; amorphous hazy proton density that extends from the right lateral margin of the first thoracic vertebra (IT) obscuring the lucency of the trachea (T) extending down over the spinous process of the second thoracic vertebra medial to the arch of the aorta (A); mediastinum widening over the right lateral margin of the manubrium (not labeled) and the ascending aorta, and the otherwise normal lungs.

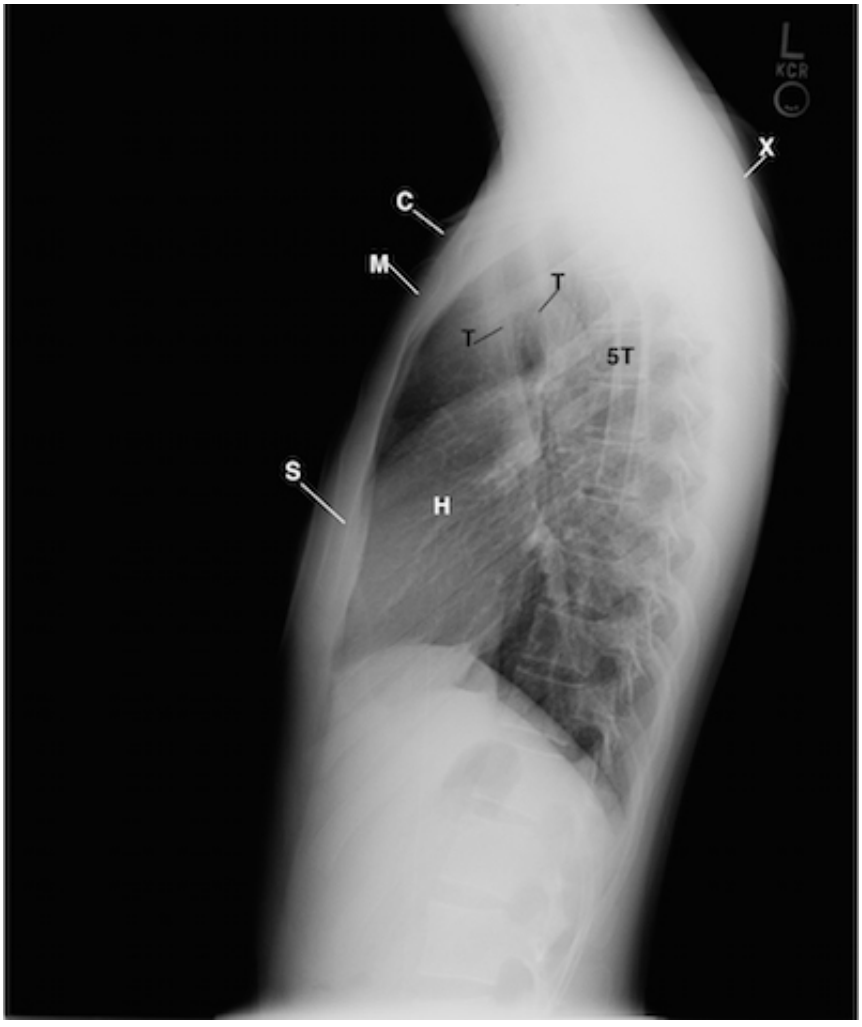

FIGURE 2. This is a lateral chest radiograph that cross references the PA chest radiograph to display the narrow thorax with the arms elevated overhead; forward shift of the cervicothoracic spine (not labeled); bilateral rounding of the shoulders (X); mild anterior bowed body of the sternum (S) with the backward displaced manubrium (M) increasing the slope of the first ribs (not labeled) with mild kyphosis of the

thoracic spine (not labeled); hazy dense obscuration of the ascending aorta (not labeled) and trachea (T) down over the first and second ribs. Clavicle (C), Heart (H), Fifth thoracic vertebra (5T).

FIGURE 3. This is a coronal image that displays thin subcutaneous tissues (not labeled); drooping right shoulder as compared to the elevated left shoulder (not labeled); low proton dense venous return thru the bulbous expanded dominant right internal jugular vein (J) reflecting costoclavicular compression of the inferior bicuspid valve within the right internal jugular vein as compared to the gray proton dense smaller left internal jugular vein (J); gray proton dense enlarged thymus gland (THY) splaying apart the brachiocephalic veins (BRV), anterior to the common carotid arteries (CC), brachiocephalic trunk (not labeled) and the ascending aorta (A). Clavicle (C), Cephalic vein (CV), Coracoid Process (CP), First rib (FR), Pulmonary artery (P), Right and Left lungs (RL, LL), Subclavius muscle (SUB), Subclavian vein (SV), Trachea (T).

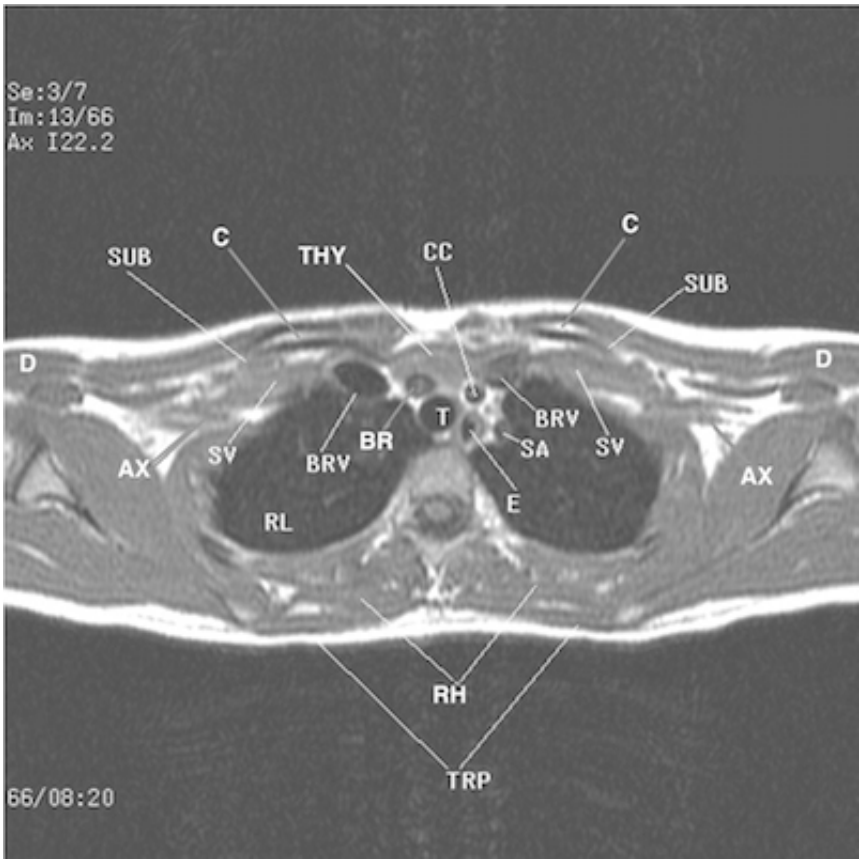

FIGURE 4. This is a transverse T1 weighted MRI image that cross references the coronal sequence to display the manubrium (not displayed) sloping posterior right placing the head of the right clavicle slightly posterior to the left (not labeled), thin subcutaneous tissues (not labeled), narrow thorax (not labeled) dominant drooping right shoulder as compared to the forward rotated left (not labeled) reflecting laxity of the sling/erector muscles, left greater than right.

Observe the gray proton dense thymus gland (THY) displacing the gray proton dense brachiocephalic trunk against the trachea (A) compressing the gray proton dense hazy left brachiocephalic vein (BRV) posteriorly. Axillary Artery (AX), Brachiocephalic Trunk (BR), Common Carotid artery (CC), Esophagus (E), Deltoid muscle (D), Right and Left Lungs (RL, LL), Rhomboid muscle (RH), Trapezius muscle (TRP), Left Subclavian artery (SA), gray proton dense bulbous expanded Subclavian Vein (SV), Trachea (T).

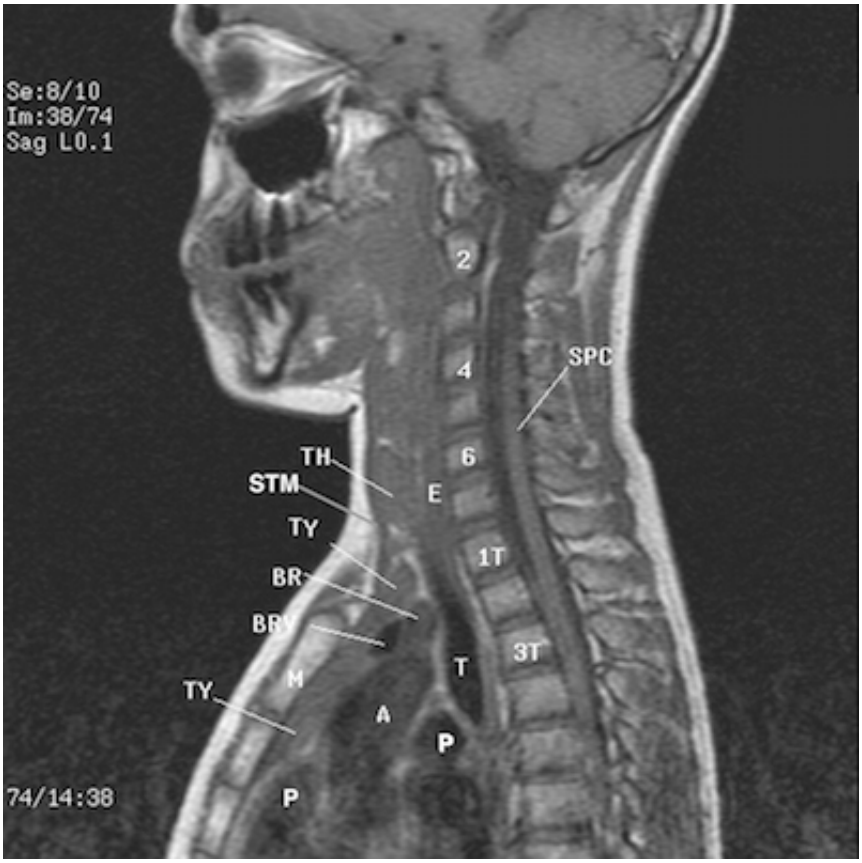

FIGURE 5. This is a left sagittal T1 weighted image that cross references the coronal and transverse sequences to display the mass effect of the backward head of the left sternocleidomastoid muscle (STM) attached to the backward manubrium (M) with the body of the sternum (S) compressing the gray proton dense thymus gland (TY) against the ascending aorta (A), pulmonary trunk (P), left brachiocephalic vein (BRV), and the dilated gray proton dense dilated brachiocephalic trunk (BR) against the against the trachea (T).

Observe the backward left sternocleidomastoid muscle compressing the fascial plane separation of the left thyroid gland (TH) and the thymus gland against the region of the esophagus (E) and trachea (T). Cervical vertebrae (2,4,6), thoracic vertebrae (1T, 3T), spinal cord (SPC).

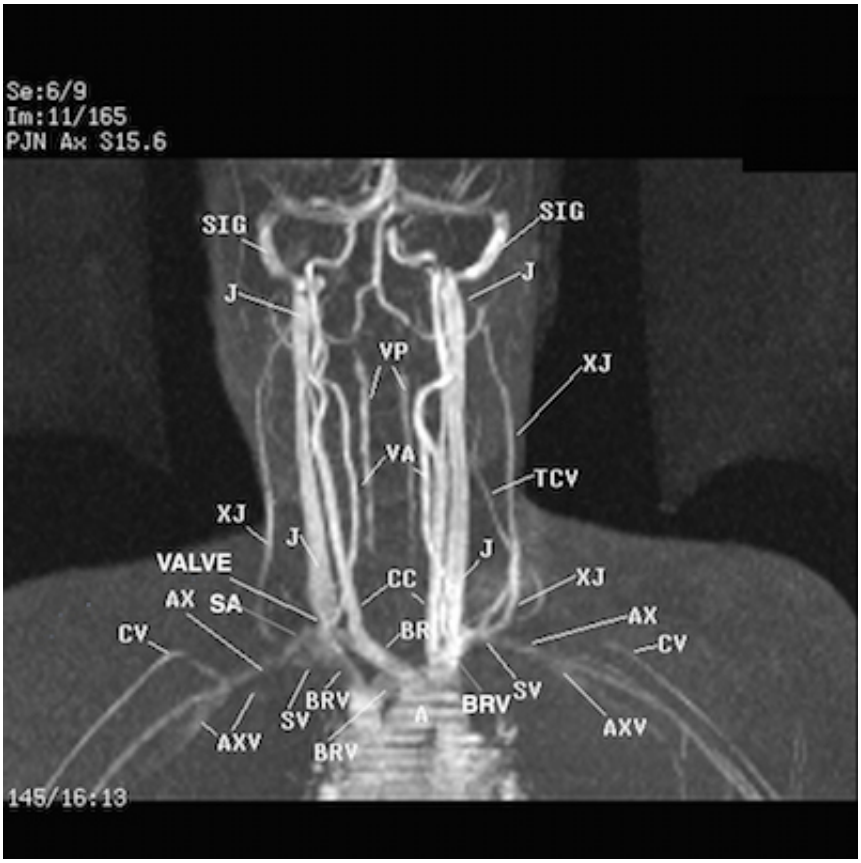

FIGURE 6. This is a 2D Time Of Flight MRA (magnetic resonance angiography); MRV (magnetic resonance venorgraphy) 3D reconstructed coronal image that confirms the T1 weighted images above. Observe the gray proton dense first division of the right subclavian artery (SA) reflecting compression of the right axillary artery compression of the right axillary vein in the right supraclavicular fossa impeding arterial flow coursing posterior to the “cone shaped” compressed region of the inferior bicuspid valve (VALVE) within the right internal jugular vein (J), and the asymmetric diminished venous return within the right and left axillary (AXV) and cephalic veins (CV); asymmetric gray proton dense compressed right brachiocephalic vein (BRV) and the gray proton dense left brachiocephalic vein medial to the formation of the high proton dense turbulence within the superior vena cava (not labeled) reflecting the thymus gland compression of the soft tissues posterior to the manubrium on the T1 weighted images of the above described sequences. The high proton densities of the left sigmoid sinus (SIG) and the left internal jugular vein (J) reflect impedance venous to return secondary to the mass effect by thymus gland. Axillary Artery (AX), External Jugular vein (XJ), Subclavian Vein (SV), Transverse Cervical vein (TCV), Vertebral Venous Plexus/Batson’s plexus (VP), Vertebral Artery (VA).

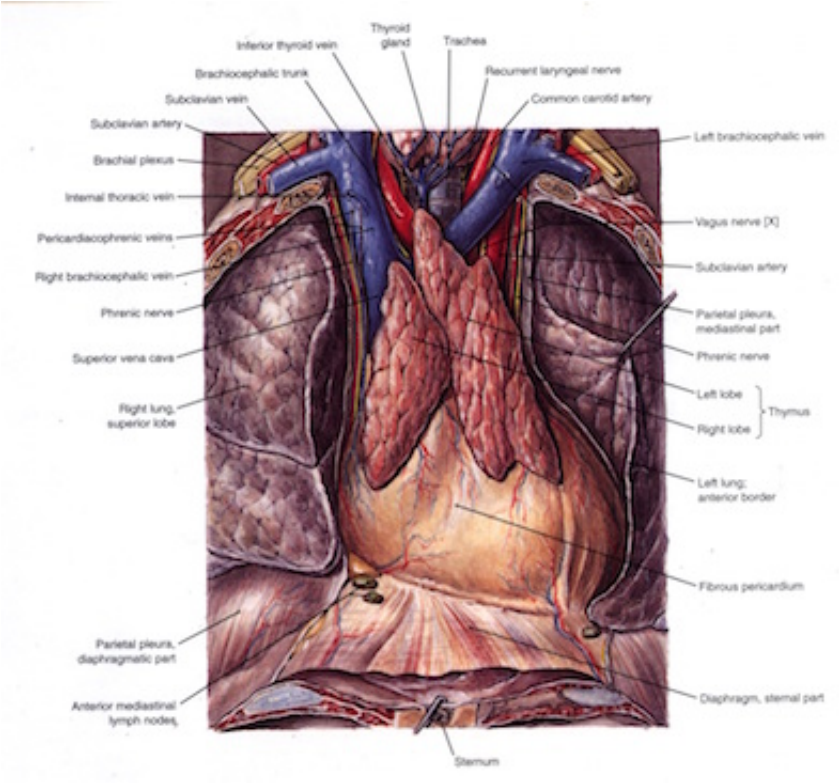

FIGURE 7. This is an image of the thymus gland within the thorax provided by permission of Clemente, C. D. 1987 Anatomy, A Regional Atlas of The Human Body. 5th Ed, Baltimore: Urban and Schwarzenberg. Observe the proximity of the thymus gland to the inferior thyroid vein that is often compressed by the backward left brachiocephalic vein in costoclavicular compression of the brachial plexus in patients with the clinical diagnosis of thoracic outlet syndrome-Hypothyroidism

REFERENCES

1) Scheuermann's disease as a model displaying the mechanism of venous obstruction in thoracic outlet syndrome and migraine patients: MRI and MRA. J Natl Med Assoc. 2003 Apr; 95(4): 298–306

2. TOSINFO.COM

3. NERVES ON MAGNETIC IMAGING. J Natl Med Assoc. VOL 81. NO 2 1989 FEB: 129-134.

4. Sunderland S. Blood supply of the nerves to the upper limb in man. Arch Neurol Psych.1945;53:91–115. ed. 2. Philadelphia, WB Saunders Co, 1984; 760–870.

5. Woodburne, RT, Burkel WE. Essentials of Human Anatomy. Ed 8th. New York, Oxford University Press 1988: 18-216.

6. Collins JD, Shaver M, Batra P, Brown K, Disher A. Magnetic Resonance Imaging of Chest Wall Lesions. J Natl Med Assoc. 1991: 4: 352-360